Numerical Investigation of Shock Tube Flow under Rarefied Conditions

D.S.Watvisave, U.V. Bhandarkar, B.P. Puranik

Department of Mechanical Engineering, Indian Institute of Technology Bombay, Powai, Mumbai-400076, India

Abstract. Two-dimensional Direct Simulation Monte Carlo (DSMC) simulations are carried out for investigating the shock wave propagation and boundary layer effects in a shock tube flow, for a wide range of rarefied conditions. Nitrogen is used for all simulations. The Cercignani-Lampis-Lord (CLL) model of gas surface interactions is implemented to study the effects of boundary layer which develops behind the moving shock front. The effect of surfaces is analyzed with different tangential momentum accommodation coefficient (TMAC) values in the CLL model. The Larsen-Borgnakke (LB) model of inelastic collisions is implemented for diatomic gases. The shock front deceleration and the contact surface acceleration phenomena due to viscous effects are studied. The simulation at higher Knudsen number flows shows disappearance of the shock front and the contact surface.

Keywords: Shock Tube Flow, Direct Simulation Monte Carlo, Rarefied Gas Flow, Micro-shock Tubes
PACS: 47.45n.07.35+k

INTRODUCTION

Recent developments in micro-mechanical and nano-mechanical devices have made it possible to use micro and macro shock tubes for novel applications such as drug delivery systems, gene therapy, wood preservation along with conventional applications in chemical kinetics and combustion studies. These advances created a renewed interest in the investigations of shock tubes operating at high Knudsen number conditions. The investigations of macro shock tubes operating at low pressures have been perfomed by several researchers. The analytical study of low pressure shock tubes was performed by Roshko [1], wherein the decrease in the flow duration time due to wall effects was established, and similarity parameters for length and flow time were developed. Duff [2] carried out experiments to study shock tubes operating at low driver pressures and observed the shock wave attenuation and the boundary layer effects. Mirels [3] further refined the results of Roshko analytically and found the boundary layer parameter for various combinations of Mach number and gases. Recently Zeitoun et al. [4] carried out numerical simulations of micro-shock tubes using kinetic equations and Direct Simulation Monte Carlo (DSMC) method to investigate boundary layer effects in monatomic gas. The objective of the present work is to investigate viscous effects and rotational relaxation of diatomic gases in shock tubes at rarefied conditions using the DSMC method. The flow duration, shock attenuation, boundary layer thicknesses for diatomic gas shock tube flows for two Knudsen numbers are studied.

RAREFIED SHOCK TUBE PROBLEM

When the Knudsen number is in the range of 0.001 to 10 in a shock tube either due to very low operating pressures or due to very small characteristic lengths, the inviscid theory of shock tubes can not be applied. At these Knudsen number flows the wall effects can not be neglected. A relatively thick boundary layer develops between the shock front and the contact surface, causing deceleration of the shock front and acceleration of the contact surface. Due to this effect the shock Mach number and the shock strength reduce significantly [2]. To study these effects with DSMC, the initial pressure in the driver section of the shock tube is kept at low values from 0.041 Pa to 41 KPa, corresponding to number densities of $1e22/m^3$ to $1e24/m^3$ at a temperature of $300K$. The diaphragm pressure ratio is chosen as 20. The gas used in all simulations on both sides of the diaphragm is Nitrogen. The domain sizes and the corresponding Knudsen numbers on the high pressure side of the shock tube are given in Table 1. At time $t = 0$ the molecules are assigned random positions and Maxwellian velocities. The molecules are allowed to move at time $t = 0$, which simulates breaking of the diaphragm. A shock wave and an expansion wave are generated in the domain as time marches.

TABLE 1. Shock Tube Test Cases

Number Density ($1/m^3$)	Pressure (kPa)	Diameter (m)	Length (m)	Driver side Knudsen Number
1e22	0.041	2e-4	1	0.6
1e22	0.041	2e-3	1	0.06
1e23	0.41	2e-4	0.1	0.06
1e24	41	2e-4	0.01	0.006

THE DSMC SOLVER

The DSMC solver used in the shock tube analysis is a two-dimensional serial code, developed in-house. For collisions, the No Time Counter (NTC) method of Bird [5] is used. The collision and sampling grids are kept identical to maintain simplicity of the code. The size of the cells on the high pressure and the low pressure side of the shock tube are different to keep optimum number of simulated molecules in each cell. The time step is kept to a value to give correct collision rate and optimal computational time. The total number of simulated molecules in the domain is increased upto 18 million depending upon the number density and domain size.

All types of gases with elastic or inelastic collisions can be analyzed with the solver. The Variable Hard Sphere model (VHS) is used to simulate elastic collisions. The Larsen-Borgnakke (LB) model [6] is used to model inelastic collisions. A provision is made to select either constant or temperature-dependent relaxation number. As the temperatures encountered in the analysis are relatively low, the vibrational excitation is not considered in the code.

The reflection of molecules from the horizontal walls of the shock tube is either specular, diffuse or a combination of both employed using the Cercignani-Lampis-Lord (CLL) model [7]. The reflection with vertical walls is specular in all cases. A provision is made to select different values of thermal momentum accomodation coefficient (TMAC) in the CLL model. The macroscopic properties are found using cumulative ensemble averaging at the end of all runs; this technique reduces false components of stream velocity to very low values, ensuring correctness of macroscopic properties.

RESULTS

Shock Wave Propagation without Wall Effects

The shock wave propagation without wall effects is studied by implementing specular reflection boundary condition at the walls. In this type of boundary condition the normal component of velocity reverses after the interaction with the wall and parallel components of velocity remain unchanged. After initialization of motion, intermolecular collisions take place and the gradients in macroscopic properties begin to develop. The pressure, density, temperature and velocity distribution along the length at various time steps for a driver side initial Knudsen number 0.6 are shown in Fig. 1 to Fig. 4. It is evident that the jump in the pressure and density across the shock is gradual. The shock thickness is of the order of few (7 to 10) mean free path lengths. The contact surface and the shock front are traveling at constant speed. The simulated Mach number of the shock front is 1.84 and the shock strength (P_2/P_1) is 3.82 for a diaphragm pressure ratio of 20, which compare well with values predicted by the inviscid shock tube theory [8] thus validating the code. The density and pressure distributions show that the position at which the shock develops, i.e., when the shock front and the contact surface are clearly separated from each other and can be distinguished, is predicted to be of the order of 100 to 200 times the mean free path in the driven region. In the absence of wall effects the flow duration, which is defined as the duration between arrival of the shock front and that of the contact surface at a point [2], goes on increasing as the shock wave travels along the length of tube.

Wall Effects with Diffuse Reflection

The behaviour of real shock tube flow differs from the ideal shock tube flow due to formation and growth of a boundary layer behind the moving shock [4, 9]. The wall effects in the DSMC analysis are introduced by diffuse reflection of the molecules with walls. The scattering kernel of the reflecting molecules is such that the normal velocity

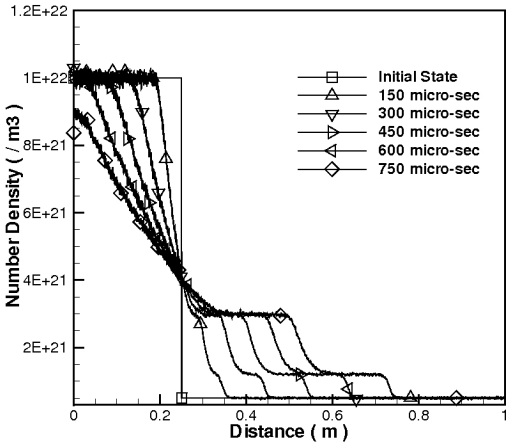

FIGURE 1. Density distribution along the length with specular reflection (Initial conditions: Kn=0.6, Driver side pressure=41Pa, Diaphragm pressure ratio=20)

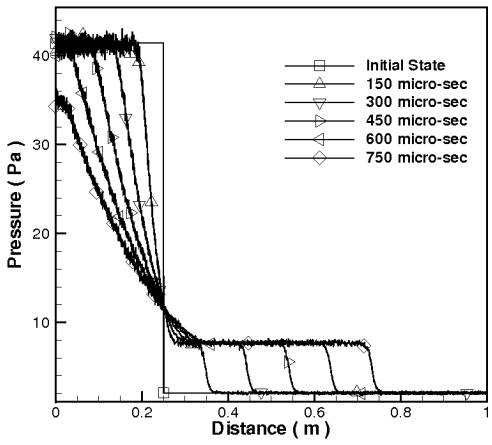

FIGURE 2. Pressure distribution along the length with specular reflection (Initial conditions: Kn=0.6, Driver side pressure=41Pa, Diaphragm pressure ratio=20)

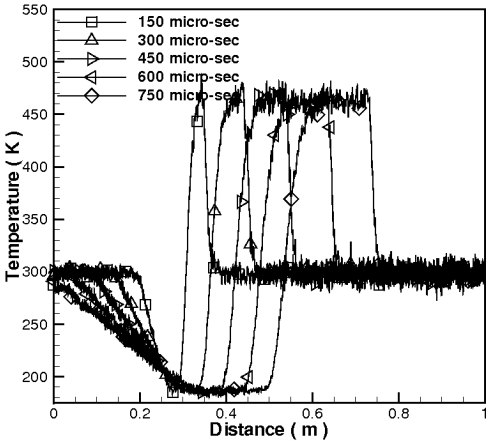

FIGURE 3. Temperature distribution along the length with specular reflection (Initial conditions: Kn=0.6, Driver side pressure=41Pa, Diaphragm pressure ratio=20)

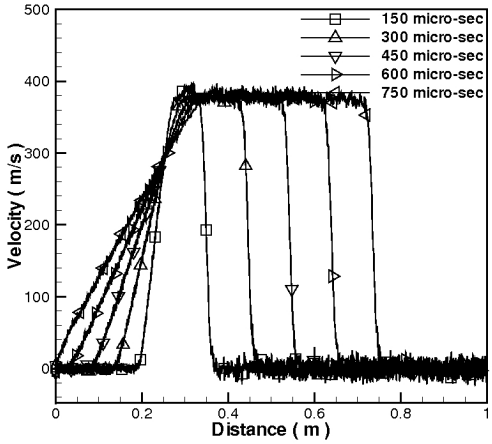

FIGURE 4. Velocity distribution along the length with specular reflection (Initial conditions: Kn=0.6, Driver side pressure=41Pa, Diaphragm pressure ratio=20)

of a molecule after reflection reverses and parallel components are allowed to take any direction in the plane of the wall. The magnitudes of velocities are sampled from Maxwellian distribution corresponding to the wall temperature.

The simulations of shock tube operating at Knudsen numbers 0.06 and 0.6 are performed in the study. The pressure distribution at Kn=0.6 and Kn=0.06 are shown in Fig. 5 and Fig. 6 respectively. The results at Kn=0.06 are consistent with the corresponding results in [4]. The shock strength and the shock Mach number have decreased significantly at both Knudsen number flows, as compared to the case with specular reflection as shown in Fig. 2. The comparison of Fig. 5 and Fig. 6 clearly shows that with an increase in the Knudsen number viscous dissipation becomes stronger. The contact surface and the shock front disappear much faster in the case with high Knudsen number, implying shock front deceleration and contact surface acceleration as discussed in [3]. The comparison of velocity distributions in

Fig. 7 and Fig. 8 clearly shows rapid decrease in the shock speed at higher Knudsen number flow. The velocity of the "shock front" at large distances from the diaphragm becomes subsonic, which strongly indicates that the wall effects are severe, due to which the shock wave completely vanishes.

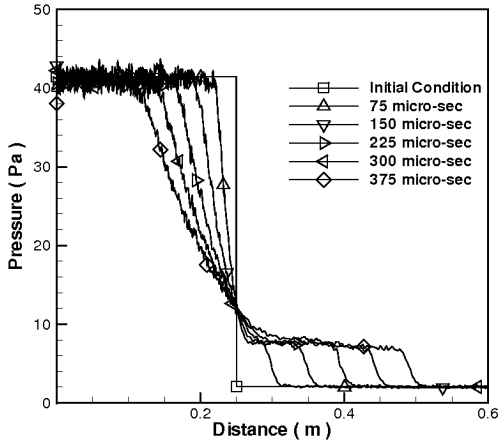

FIGURE 5. Pressure distribution along the length with diffuse reflection (Initial conditions: Kn=0.06, Driver side pressure=41Pa, Diaphragm pressure ratio=20)

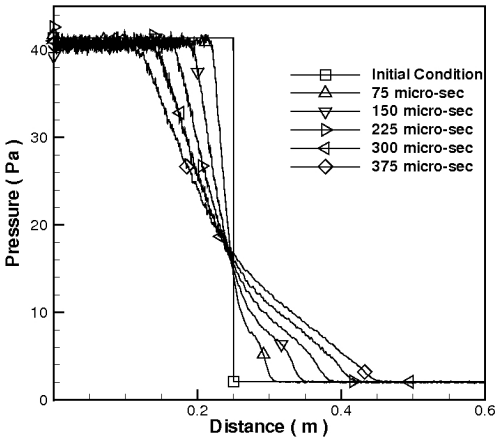

FIGURE 6. Pressure distribution along the length with diffuse reflection (Initial conditions: Kn=0.6, Driver side pressure=41Pa, Diaphragm pressure ratio=20)

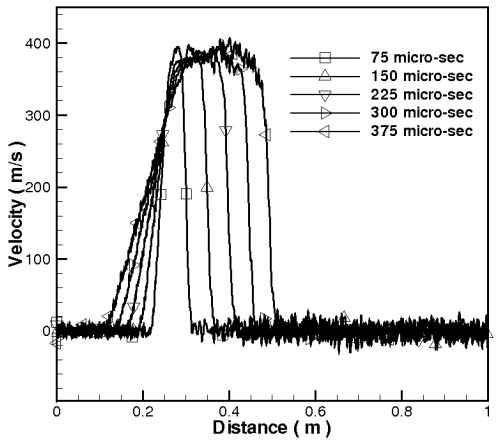

FIGURE 7. Velocity distribution along the length with diffuse reflection (Initial conditions: Kn=0.06, Driver side pressure=41Pa, Diaphragm pressure ratio=20)

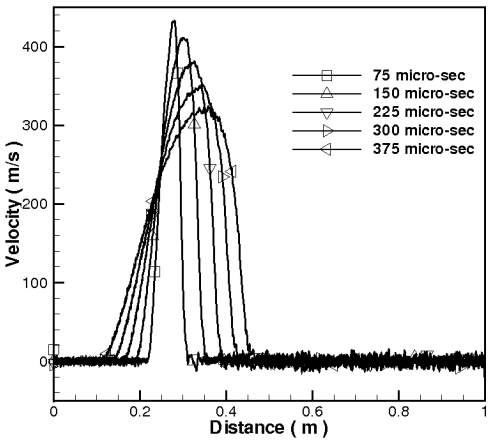

FIGURE 8. Velocity distribution along the length with diffuse reflection (Initial conditions: Kn=0.6, Driver side pressure=41Pa, Diaphragm pressure ratio=20)

Wall Effects with CLL Reflection

When the flow is supersonic, the time for a molecule to be in complete equilibrium with walls is less. As a consequence the reflection of the molecules is expected to take place with incomplete accommodation. The gas surface interaction with incomplete accommodation is implemented using the CLL Model. In the CLL model there is no coupling between the normal and parallel velocity components. The distribution functions of normal and tangential components of velocities after interaction with the walls are given in [7].

The TMAC equal to zero corresponds to specular reflection and the TMAC equal to one corresponds to diffuse reflection in the CLL model. Hence to study the wall effects in which the gas molecule interacts with the wall with incomplete accommodation, the values of TMAC are selected between 0.2 to 0.8. The Knudsen number of the flow is chosen as 0.6 and the diaphragm pressure ratio is 20. The density and velocity distributions are shown in Fig. 9 and Fig. 10, at a time step of 375 micro-seconds after the rupture of the diaphragm. As TMAC increases, the viscous dissipation increases, decreasing the shock front speed and increasing the contact surface speed for the same value of the Knudsen number. The variation in the flow properties is sensitive to the selection of the TMAC value in the CLL model. The correct value of TMAC can be selected by comparing the simulated and experimental results or performing molecular dynamics simulation for shock tubes.

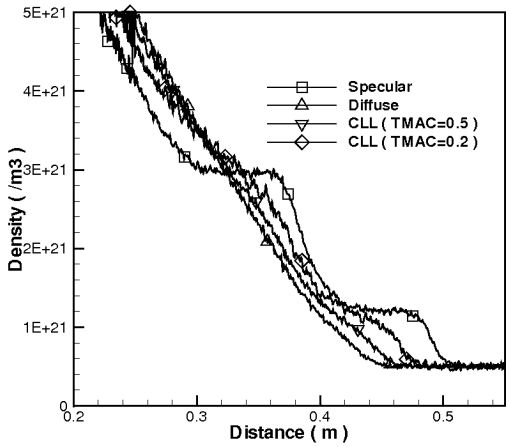

FIGURE 9. Desnsity distribution at time step 375 micro-sec (Initial conditions: Kn=0.6, Driver side pressure=41Pa, Diaphragm pressure ratio=20, TMAC =0.2, 0.5)

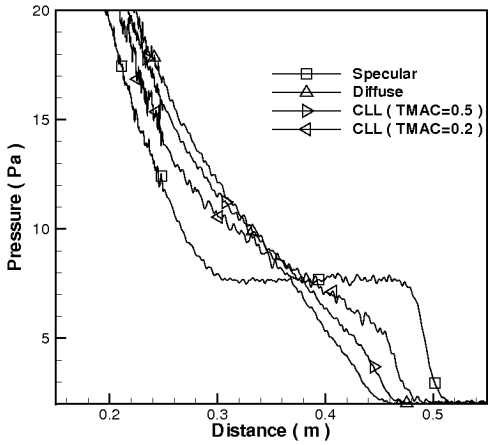

FIGURE 10. Pressure distribution at time step 375 micro-sec (Initial conditions: Kn=0.6, Driver side pressure=41Pa, Diaphragm pressure ratio=20, TMAC =0.2, 0.5)

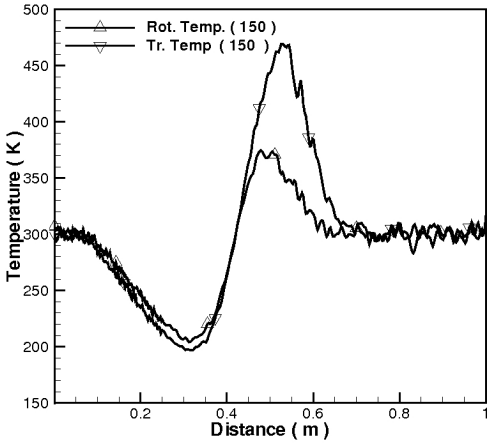

FIGURE 11. Rotational and translational temperature at 150 micro-sec after diaphragm rupture with specular reflection (Initial conditions: Kn=0.6, Driver side pressure=41Pa, Diaphragm pressure ratio=20)

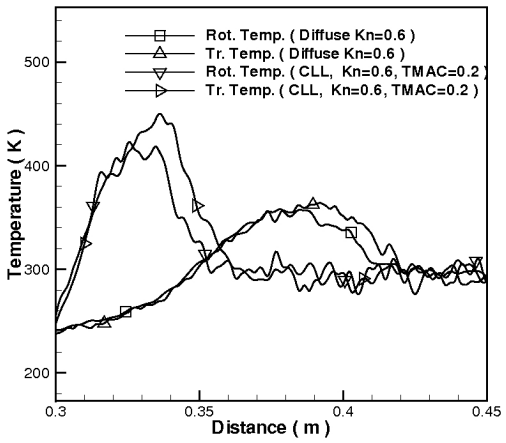

FIGURE 12. Rotational and translational temperature at 150 micro-sec with CLL reflection (TMAC=0.2) and 300 micro-sec with diffuse reflection (Initial conditions: Kn=0.6, Driver side pressure=41Pa, Diaphragm pressure ratio=20)

Rotational Relaxation in Shock Tube

The rotational relaxation in the propagating shock wave is investigated using the Larsen-Borgnakke model of inelastic collisions [6]. The rotational collision number which is defined as a measure of the average number of collisions which a polyatomic gas molecule experiences in rotational-translational energy exchange is selected as a constant value (equal to 5) given for the gas under study from [5]. The rotational relaxation is studied with specular reflection and the results are compared with those in [5]. After validating the LB model for specular case, it is extended to gas-surface interaction with diffuse reflection and with CLL reflection.

The rotational and translational temperature distributions along the length of shock tube after the diaphragm rupture are shown in Fig. 11 and Fig. 12. The results show that the rotational temperature lags behind the translational temperature inside the shock front in all cases. The viscous dissipation causes a decrease in the rotational temperature jump similar to that in the translational temperature.

CONCLUSION

A shock tube flow is investigated to study the wall effects on shock wave propagation using DSMC. The DSMC solver is developed and validated with one-dimensional shock tube theory [8]. The boundary layer effects are futher investigated with diffuse reflection and reflection with the CLL model. The shock tube flow with two different Knudsen numbers is simulated for the diffuse reflection case. The contact surface acceleration and the shock front deceleration are observed in the flows with Kn in the slip regime flow and Kn in the transition regime flow, consistent with the results in [4]. The flow with higher Knudsen number shows rapid disappearance of shock front and contact surface.

The application of CLL model of gas-surface interaction with different values of TMAC revealed that, in case of TMAC values less than 0.5, the viscous effects are less dominant than those in diffuse reflection. The distinct shock front and contact surface remain in the flow for longer time. For relatively high speed flows, molecules are expected get less time to accommodate with the wall, and may most probably reflect with lower TMAC values. Hence the selection of correct value of TMAC is a key factor in predicting correct flow physics of the rarefied shock tube flow. A better approach to the rarefied shock tube flow analysis is to carry out a number of simulations at different values of TMAC and to compare these results with available experimental results to determine the correct value of TMAC. Since experimental observations appear to be scarce in rarefied shock tubes, molecular dynamics simulations are planned to determine the exact TMAC values.

The investigation of rotational relaxation for all types of gas-surface interactions shows that the rotational temperature lags behind the translational temperature inside the shock wave. The rotational and translational temperature are in equilibrium away from the shock region.

REFERENCES

1. A. Roshko, *Physics of Fluids* **3**, 835–842 (1960).
2. R. E. Duff, *Physics of Fluids* **2**, 207–216 (1959).
3. H. Mirels, *Physics of Fluids* **6**, 1201–1214 (1963).
4. D. E. Zeitoun, Y. Burstschell, I. A. Graur, M. S. Ivanov, A. N. Kudryavstev, Y. A. Bondar, *Shock Waves* **19**, 307–316 (2009).
5. G. A.Bird, *Molecular Gas Dynamics and Direct Simulation of Gas Flows*, Oxford University Press, Oxford , 1994.
6. C. Borgnakke, P. S. Larsen, *Journal of Computational Physics* **13**, 405–420 (1975).
7. R. G. Lord, *Physics of Fluids* **7**, 1159–1161 (1995).
8. M. A. Saad, *Compressible Fluid Flow*,Prentice Hall, New Jersy , 1985.
9. G. Mirshekari, M. Brouillete, *Shock Waves* **19**, 25–38 (2009).